

# Faraday rotation in magnetic colloidal photonic crystals

Wim Libaers<sup>a</sup>, Branko Kolaric<sup>a,b</sup>, Renaud A. L. Vallée<sup>a,c</sup>, John E. Wong<sup>d</sup>, Jelle Wouters<sup>a</sup>, Ventsislav K. Valev<sup>a</sup>, Thierry Verbiest<sup>a</sup>, Koen Clays<sup>a</sup>

<sup>a</sup> Department of Chemistry, K.U. Leuven and Institute of Nanoscale Physics and Chemistry (INPAC), Celestijnenlaan 200D, 3001 Heverlee, Belgium.

<sup>b</sup> Laboratoire Interfaces & Fluides Complexes, Centre d'Innovation et de Recherche en Matériaux Polymères, Université de Mons Hainaut, 20 Place du Parc, B-7000 Mons, Belgium

<sup>c</sup> Centre de Recherche Paul Pascal (CNRS) - 115, avenue du docteur Schweitzer - 33600 Pessac - France

<sup>d</sup> RWTH Aachen University, Institute of Physical Chemistry, Landoltweg 2, 52056 Aachen, Germany.

## ABSTRACT

Faraday rotation for magnetic field sensing can find applications in satellite altitude monitoring. Enhancing and tuning Faraday rotation is demonstrated in hybrid magnetic photonic crystals, based on an independent nanoscale engineering of two different materials (silica and iron oxide) at different length scales (< 20 and > 200 nm). An engineering approach towards combined photonic band gap properties and magnetic functionalities, based on independent nanoscale engineering of two different materials at different length scales, is conceptually presented, backed by simulations, and experimentally confirmed. Large (> 200 nm) monodisperse nanospheres of transparent silica self-assemble into a photonic crystal with a visible band gap, which is retained upon infiltration of small (< 20 nm) nanoparticles of magnetic iron oxide. Enhancing and tuning Faraday rotation in photonic crystals is demonstrated.

**Keywords:** photonic crystals, magnetic colloids, Faraday rotation, maghemite, superparamagnetic

## 1. INTRODUCTION

### 1.1 The importance of magnetic nanomaterials

Magnetic nanoparticles are an important part of many current technologies, and new applications for them continue to be developed in such diverse fields as magnetic fluids, drug delivery, catalysis and magneto-optic data storage.<sup>1-8</sup> Given their importance and wide applicability, many methods for their preparation have been developed.<sup>1-4,9-11</sup> The size of these particles is an important factor in determining their magnetic properties. Nanoparticles in the range of 5-25 nm exhibit superparamagnetic behaviour, where every nanoparticle will be a single domain, behaving like a giant paramagnetic atom, having a fast response with negligible remanence to externally applied fields.<sup>1</sup> We intend to use such superparamagnetic particles, made of iron oxide, to design photonic crystals (PCs) with enhanced magneto-optical properties.

Photonic crystals are a relatively new class of materials (though some of these structures are found in nature<sup>12</sup>) designed to have a periodically varying refractive index on a size scale similar to that of the wavelength of the light one wishes to control.<sup>13</sup> This periodicity can be realized in one, two or three dimensions. These structures can block the propagation of light of specific frequency ranges at certain angles by the creation of a photonic band gap, analogous to the band gap in semiconductors. Such structures can be made using a top-down or bottom-up approach.<sup>14</sup> In the top-down approach, one designs systems to be fabricated by planned removals and additions of materials in a specific geometry, for example by drilling a pattern of holes in a dielectric, or using nanolithography at smaller scales. Such top-down techniques become increasingly challenging when the required sizes become smaller, which is why much research on photonic crystals for the visible light range is done using a bottom-up approach instead. A convenient way to produce a class of 3D photonic crystals known as synthetic opals consists of ordering, through convective self-assembly,<sup>15,16</sup> Langmuir-Blodgett deposition,<sup>17,18</sup> sedimentation<sup>19</sup> or spin-coating<sup>20,21</sup> of monodisperse, colloidal spheres in colloidal crystals. The spectral position, width and amplitude of the band gap in these systems is a function of the size of the colloidal spheres and of the

refractive index of the materials used in the close-packed (filling fraction 0.74) fcc, hcp or rhcp crystal structures obtained by this technique. It should also be noted that the band gap in this type of photonic crystal is not a complete, omnidirectional band gap, but has some angular dependence, a property we exploit in this study.

The engineering of a photonic band gap material with magnetic functionality is one of the major goals in the field of optical materials since magnetic materials can be used for additional control of the properties of light e.g. nonreciprocal effects in the magnetic PCs.<sup>22,23</sup> Nonreciprocity, which is a known feature of magnetic photonic crystals,<sup>24</sup> includes the possibility of unidirectional propagation of light. The use of magnetic particles with a high refractive index, like iron oxide particles, must also lead to an enhancement of the photonic band gap effect, in addition to the magnetic effects expected under application of an external magnetic field.<sup>25,26</sup>

Another reason to investigate such materials is their application in magnetic sensor technology. Sensors based on the magneto-optical effect, or Faraday effect, have considerable advantages due to their extremely fast response and the fact that no electrical connections need to be made to or near the active material of the sensor, thus avoiding interference and sometimes safety issues. Unfortunately, their sensitivity is rather poor compared to many other magnetic sensing technologies because the Faraday rotation is rather small for fields comparable to the earth's magnetic field.<sup>27</sup> If materials can be found where this effect is much larger, this type of sensor may become a very useful component of vector magnetometers for navigation in the earth's field and remote sensing.<sup>28</sup>

## 1.2 Development of composite silica-maghemite colloids for magnetophotonics.

The use of superparamagnetic iron oxide poses two main challenges when applied to photonic crystal design. First, the size of approximately 10 nm is far too small to produce a bandgap in the visible region. Second, the material is highly absorbing in the bulk, and therefore by itself not practical to use in optical applications. We pursued several strategies to integrate the magnetic particles into the well-established self-assembly of synthetic opals using monodisperse silica colloids. Initial attempts focused on the use of superparamagnetic particles as seeds for the growth of a silica shell using the Stöber method.<sup>29</sup> The composite particles, however, were neither spherical nor monodisperse. The polydispersity of the core and aggregation made the resulting particles too irregular for use in photonic crystals,<sup>30</sup> as clearly observed using SEM imaging (Fig. 1).

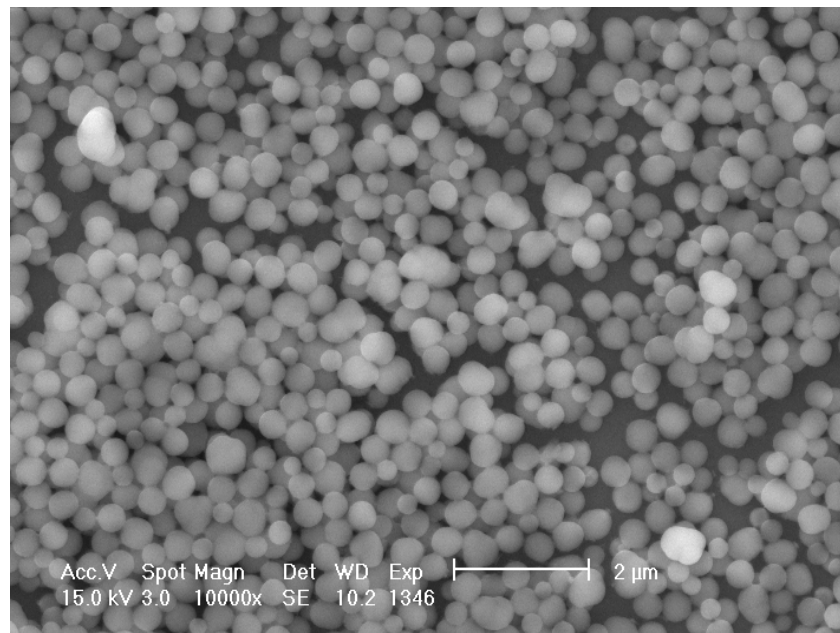


Fig. 1. SEM image of the iron oxide core – silica shell particles. The irregular shape of the individual particles and lack of ordering in the layers is clearly visible.

Another method can be used to achieve ellipsoidal particles of this type which are monodisperse enough to be used in the self-assembly method.<sup>31</sup> This involves the growth of core-shell particles using a nonmagnetic iron oxide, followed by reduction and partial oxidation of the core through the silica shell. These particles are ferromagnetic at 300 K.

A second approach we used was the addition of an iron oxide nanoparticle shell on top of monodisperse, spherical silica. To this end, the silica particles were functionalized with a linking agent, to covalently bind the iron oxide particles to the surface. In initial experiments, the iron oxide was attached before self-assembly. While this was easily accomplished, these particles failed to self-assemble into well-ordered PCs. This method did pave the way for a successful composite photonic crystal, which was created by self-assembly of silica particles with only the linking agent attached, and binding the iron oxide nanoparticles only after the crystal was formed. This eliminated any chance of the iron oxide blocking the formation of the regular structure we needed. These crystals were analysed using normal, linear transmission spectroscopy and Faraday rotation to check for magneto-optical effects.

## 2. EXPERIMENTAL PART

### 2.1 Chemical synthesis

The preparation of acid-stabilized maghemite colloids was performed based on an existing procedure.<sup>9,10</sup> A solution of 16 mmol FeCl<sub>3</sub> and 8 mmol FeSO<sub>4</sub> in 200 ml of pure water was stirred at 500 rpm, and a 13.5 ml of 25% NH<sub>3</sub> aqueous solution was added rapidly to form black particles (magnetite), which were quickly precipitated using a permanent magnet. The supernatant was decanted, and the colloids were resuspended using 20 ml of 2M nitric acid. Subsequently a solution of 10 mmol Fe(NO<sub>3</sub>)<sub>3</sub> in 30 ml of water was added, and the suspension was stirred at 80 °C for 1 hour to oxidize the particles to maghemite. The particles were then washed twice with 50 ml of 2 M nitric acid, and finally resuspended in 40 ml of water.

The Stöber method<sup>29</sup> was used to prepare silica colloids of approximately 200, 260 and 385 nm diameter. These were coated by functionalization with 3-mercaptopropyltrimethoxysilane (MPTMS),<sup>9,10</sup> by mixing 30 ml of a 1 mass % silica particle suspension in ethanol, with 0.5 ml MPTMS (85%) and 0.8 ml NH<sub>3</sub> 25% in water. This mixture was stirred vigorously for 45 minutes, and then the temperature was raised to 76 °C to distill off about one third of the ethanol. The remainder was then cooled and washed by centrifugation, the supernatant decanted, and the particles resuspended. This procedure was repeated twice with ethanol, then twice with water.

Coating the functionalized silica particles with the iron oxide particles was done by mixing equal volumes of the silica and maghemite suspensions obtained above and shaking strongly for one day. Then, excess iron particles were removed by repeatedly allowing the silica to settle under gravitational force and decanting the supernatant, which was replaced each time with clean water. For the fabrication of PCs, the water was replaced by ethanol.

Convective self-assembly was used for the preparation of colloidal crystals from these suspensions<sup>30,32</sup>. This procedure is already well-established for unfunctionalized silica particles.<sup>15,33</sup> It is performed by putting a clean glass substrate vertically in a vial containing the ethanolic colloid suspension, and letting the solvent evaporate at a fixed temperature, typically at 33 °C in our experiments. We used piranha acid (2/3 sulfuric acid, 1/3 hydrogen peroxide) to clean the glass substrate and the vial containing the suspension prior to use.

### 2.2 Methods and equipment

Imaging of the particles was done using SEM (Philips Scanning Electron Microscope XL30 FEG). In order to make the surface conductive, a thin layer of gold was sputtered onto the sample.

Optical extinction spectra were performed on large areas (millimeter sized) to ascertain the quality and spectral features of the samples using a Perkin-Elmer Lambda 900 UV-VIS-NIR spectrophotometer. The vertical axis for these spectra uses a logarithmic scale, defined as: extinction =  $-\log_{10}(\text{fraction of light transmitted})$ .

Small angle X-ray scattering (SAXS) measurements were carried out on a S-Max3000 system with a MicroMaxTM-002+ X-ray microfocus generator (Rigaku). The Bayesian weighted distance distribution function  $p(r)$  was calculated from the angle-dependent scattering using a fit routine included in the manufacturer-supplied software.<sup>34</sup>

TEM images were provided to us through a cooperation with the Max Planck Institute of Colloids and Interfaces (MPI KGF Golm, Germany).

Faraday rotation was measured at a wavelength of 830 nm on two homemade experimental setups,<sup>35,36</sup> using either a CW diode laser or a Spectra Physics Mai Tai tunable femtosecond pulsed Ti:Sapphire laser.

Simulations were performed with the finite-difference time-domain (FDTD) method,<sup>37</sup> using a freely available software package with subpixel smoothing for increased accuracy.<sup>38</sup>

In all simulations, the colloidal crystals have been represented by monodisperse silica spheres of given size (refractive index of 1.45) arranged along a cubic face centered lattice, i.e. with a packing fraction of 74%. Theoretical calculations were done assuming that the deposition of maghemite was layered, meaning that silica spheres are surrounded by maghemite shells. The filling of the pores (which could be up to 26%) with maghemite (refractive index of 2.42) has been implemented by underfilling the opal with spheres of larger size than the silica ones, but centered at the same positions, thus featuring an underlying interpenetrated maghemite network.

The computational cell, in which the incoming wave propagates along the  $z$  direction, has been implemented with periodic boundary conditions in the  $x$  and  $y$  directions and perfectly matched layers (PMLs) in the  $z$  direction. The resolution of the grid has been refined such that the convergence of the results was insured.

### 3. RESULTS AND DISCUSSION

#### 3.1 Iron oxide particles

Figure 2a shows a TEM image of the iron oxide particles. The polydispersity of these particles is clearly visible, with an average size of the iron particles determined to be approximately 10 nm. Figure 2b shows the pair distance distribution function (PDDF) of the iron oxide particles obtained by SAXS. The unsymmetrical shape of the curve suggests that the iron oxide particles are not spherical but more likely to be close to a prolate ellipsoid.<sup>39</sup>  $D_{\max}$ , defined as the maximum distance within the particle, is about 26.5 nm. From the curve fitting, using a Bayesian weighted inverse Fourier transform,<sup>34</sup> a radius of gyration  $R_g$  of  $\sim 8$  nm was calculated for the iron oxide particles. The scattering profile also shows that the particles are highly polydisperse with a mean value around 8 nm. The size of our iron oxide suggests that the particles are superparamagnetic.<sup>30</sup> Note that the TEM images are in excellent agreement with data obtained by SAXS (between 8 to 10 nm).

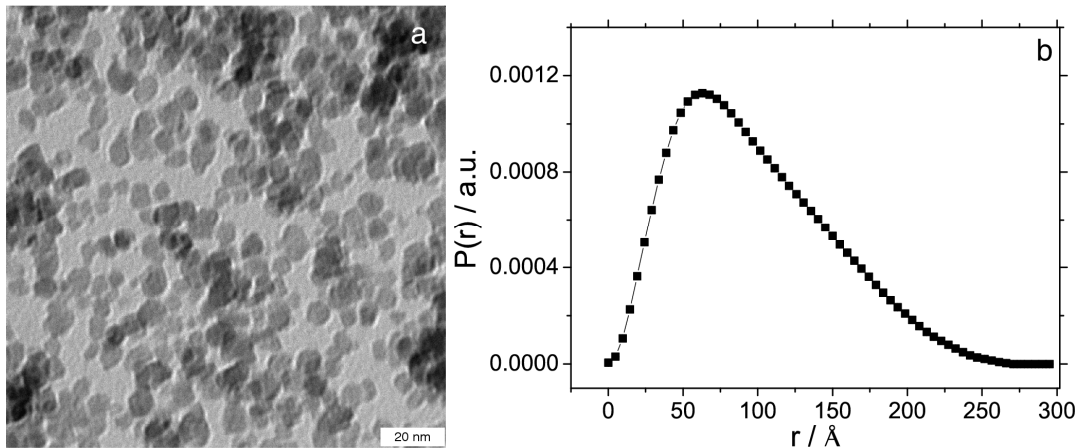


Fig. 2. (a) TEM image of the iron oxide particles. (b) pair distance distribution function of the same iron oxide particles obtained by SAXS.

#### 3.2 Iron oxide shells around silica particles

Because these magnetic particles themselves are too small for photonic applications and due to the lack of transparency, they have to be combined with another material to impart the required structural (monodisperse nanospheres at the optical wavelength scale) and optical properties (transparent). As described before,<sup>30</sup> the high polydispersity of the magnetic particles did not allow us to use iron oxide as a core for a shell of silica in order to produce monodisperse core-shell particles.<sup>30</sup> Therefore, the opposite ordering was attempted, by covalently functionalizing iron oxide particles on top of monodisperse silica spheres. Figure 3a shows a TEM image of iron oxide particles bound to the surface of silica particles. These silica/iron oxide coated particles were used in an attempt to fabricate PCs. Surprisingly these monodisperse hybrid particles can not produce a highly ordered colloidal crystal as we can see in the SEM image (Figure 3b). Two factors may be responsible for this lack of long-range ordering. The most plausible factor is surface roughness which causes steric hindrance between colloids. A second non-negligible factor to be taken into consideration is the presence of magnetic interactions between the magnetic shells. Both of these factors may be responsible for the reduced ordering quality of the crystals made from these hybrid particles, as compared to crystals obtained from bare silica

particles. As expected for unordered layers, optical transmission measurements on these multilayers (Figure 4, black dashed line) do not show a photonic band gap, but a curve that can be explained by a combination of the scattering and the absorption of the iron oxide, both increasing towards shorter wavelengths.

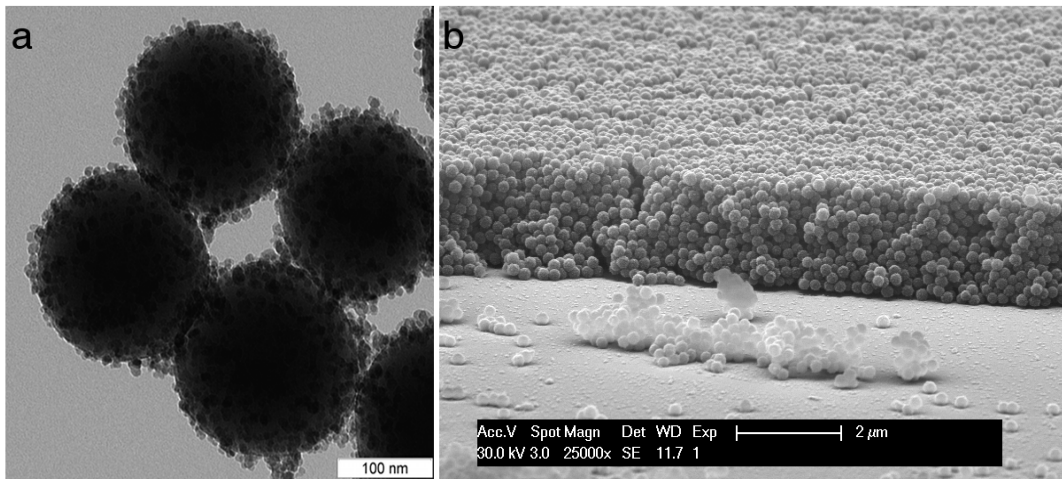


Fig. 3. (a) TEM image of the silica core – iron oxide shell particles. (b) SEM image of a multilayer of these particles. The lack of ordering in the layer is clearly visible.

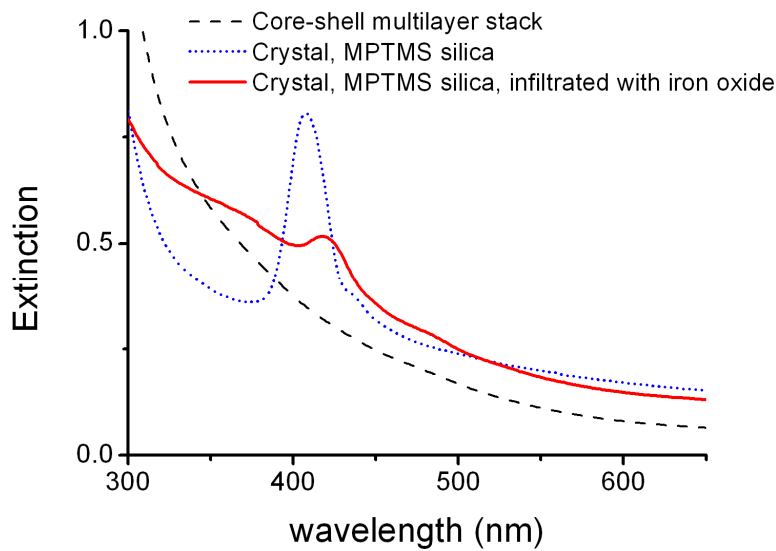


Fig. 4. Extinction spectra recorded in absorbance mode (i.e. the vertical axis is logarithmic). No photonic band gap is observed in a transmission spectrum taken from the film in Fig. 3b (black dashed lines). The dotted blue line shows the spectrum of a crystal made from MPTMS coated silica colloids, without iron oxide. The solid red line shows the spectrum of such a crystal after infiltration with iron oxide particles.

### 3.3 Well-ordered crystals including magnetic nanoparticles

The successful approach used the MPTMS-functionalized particles used in above to grow a crystal using convective self-assembly. These crystals show a band gap (Figure 4, dotted line) with a peak at 408 nm, in good agreement with the known particle size (200 nm diameter). When these crystals were infiltrated with the iron oxide suspension for one hour, then rinsed with water, iron particles remained bound due to the presence of the MPTMS. The resulting crystal shows good ordering in SEM imaging (Figure 5) and exhibits a band gap in the blue region of the visible spectrum (Figure 4a, solid line), albeit less pronounced than prior to infiltration, in addition to a strong absorption of light in the UV region due to iron oxide. The shift of the band gap to a slightly longer wavelength can be explained by the introduction of a high

refractive index material filling some of the pores in the crystal, thereby increasing the average index of the structure, while the lattice constant remains the same. This demonstrates the feasibility of fabricating photonic crystals with magnetic functionalities using this method.

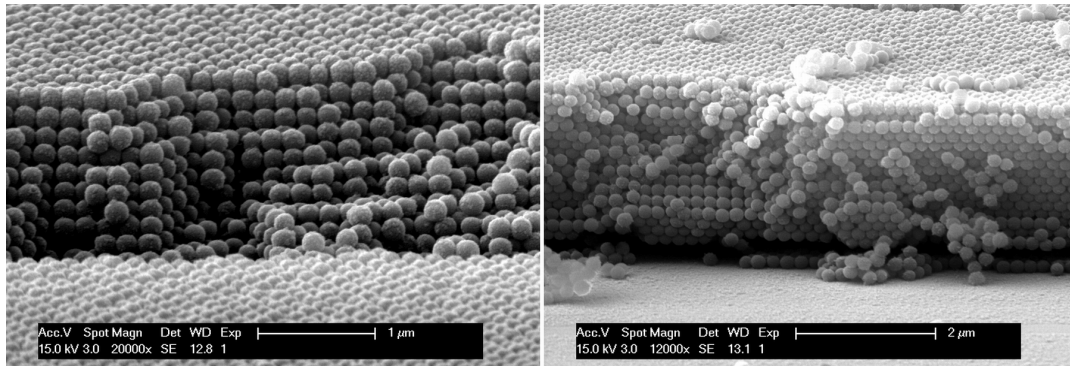


Fig. 5. SEM images of the crystal that was infiltrated with iron oxide particles after fabrication.

Both of the changes in the transmission spectrum observed on infiltration, a shift to longer wavelength and decreased height of the peak, are reproduced by simulations of a photonic crystal where the voids between the spheres ( $n=1.45$ ) are gradually filled with a material having a higher index of refraction ( $n=2.42$ ). These simulation results (Figure 6) show an increase of the wavelength where the band gap occurs and a decreased peak height as the amount of iron oxide in the voids is increased. This explains why we experimentally observe a smaller band gap even though SEM images show good ordering was retained. The simulation also shows the peak becoming bigger again when very large amounts of iron oxide are included, but our infiltration experiments did not reach this point.

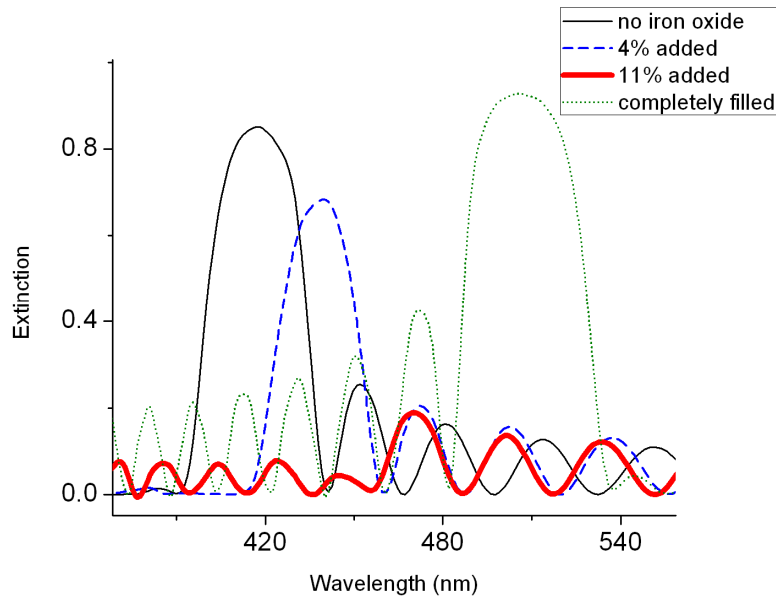


Fig. 6. Simulated transmission spectra showing the effect of increasing amounts of iron oxide in the voids, starting with the silica photonic crystal without iron oxide. A small addition of iron oxide causes a band gap shift without much reduction of the peak. At 11% iron oxide (the red line) the band gap almost disappears, to reappear at even longer wavelengths when more iron oxide is introduced until the crystal is completely filled..

Further confirmation of these results was obtained by making photonic crystals from larger silica colloids and infiltrating them with the same iron oxide particles. Such crystals have their band gap at longer wavelengths. When binding iron oxide to the surface of a functionalized silica particle, it is expected that the amount of iron oxide bound will be proportional to the surface area of the particle. Or, in the case where crystals are infiltrated, proportional to the surface

area of the voids in the crystal. If, then, the infiltration experiment is performed with crystals made of larger spheres, the volume of iron oxide that will be bound inside the voids, compared to the volume of the unit cell, is expected to become smaller and one would expect results corresponding to the simulations of smaller additions of iron oxide, i.e. a smaller wavelength shift and peak heights similar to those of the original crystal. Transmission spectra confirming this for crystals made using two different colloid sizes are shown in Figure 7, which shows both of the crystals using larger colloids before and after infiltration. We also note the pronounced increase in absorption for the infiltrated crystal with band gap at 578 nm, caused by the high optical extinction of the iron oxide at short wavelengths. The much sharper increase of absorption below 500 nm for the crystals with band gap at 837 and 847 nm is however attributed to higher order peaks of the crystal.

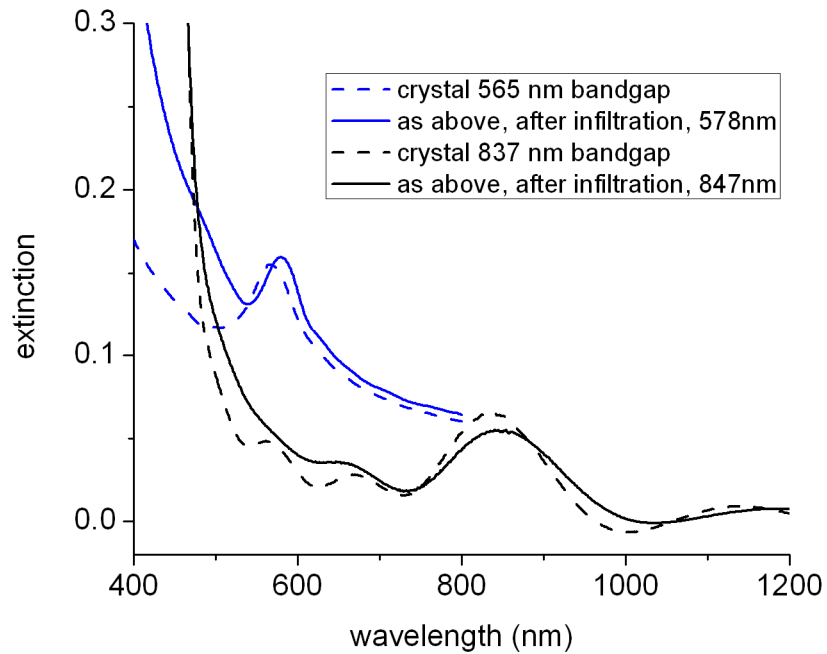


Fig. 7. Photonic crystals with band gaps at 565 and 837 nm (dashed lines), shifting to 578 and 847 nm (solid lines) after infiltration with iron oxide. Only minor amplitude changes are observed, as expected for relatively small amounts of iron oxide compared to the spectrum shown for the infiltrated in Figure 4.

To demonstrate the effect of magnetic fields on the optical properties of these crystals, Faraday rotation measurements were performed. Initial measurements<sup>40</sup> were done on an experimental setup using a CW laser at 830 nm.<sup>35,36</sup> This system is shown in Figure 8. Faraday rotation data of the photonic crystal before and after infiltration, measured at 830 nm are shown in Figure 9. AC magnetic fields up to 4 Gauss were applied to the sample, ensuring that we stay well below saturation for the magnetic particles. The data show the results of averaging over 4 experiments. The constant background due to the glass substrate was subtracted. After insertion of the magnetic nanoparticles, the specific Faraday rotation of the photonic crystal shows a substantial increase compared to the non-infiltrated crystal. Each sample was measured for incidence angles ranging from 0 to 40 degrees to study the effect of the band gap position for these incomplete band gaps. For these colloidal crystals, which do not exhibit an omnidirectional band gap, the band gap shifts to shorter wavelengths as the sample is rotated away from the perpendicular direction.<sup>16</sup> This means that we can use sample rotation as a way to measure both in and out of the band gap on the same sample. At larger angles, where the band gap is below 830 nm, the Faraday rotation appears to increase even more. The other crystals were not measured using this method, because we had no lasers with a suitable wavelength available.

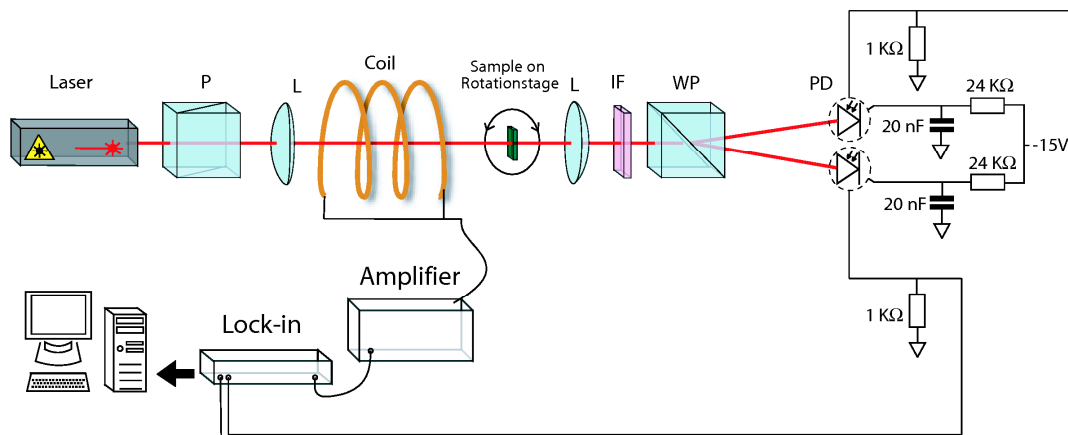


Fig. 8. Experimental setup for Faraday rotation. After passing the polarizer P, the 830 nm laser beam is focused on the sample, mounted on a rotation stage, by a lens L. It is then collimated with a second lens and then traverses an interference bandpass filter IF. Finally, it is directed through the Wollaston prism WP, set at an appropriate angle, at the photodiodes (PD). The lock-in drives the magnetic coil through the amplifier and detects the signal from the PD in phase and at the same frequency.

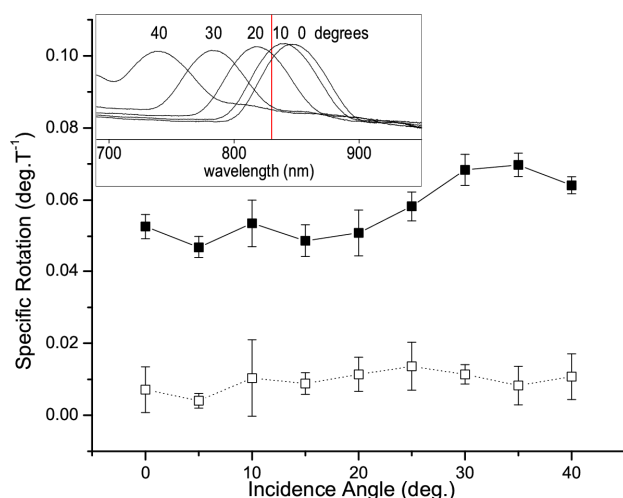


Fig. 9. Results from Faraday rotation measurements at 830 nm on the photonic crystal with band gap at 837 nm (before infiltration with iron oxide particles, open squares) and 847 nm (the same crystal after infiltration, solid squares), with the sample rotated from 0 (perpendicular to the laser beam) to 40 degrees. The inset shows the shift of the band gap to shorter wavelengths from 0 to 40 degrees in ten degree steps with the laser line at 830 nm indicated by a vertical line.

We investigated this crystal further using a tunable femtosecond pulsed Ti:Sapphire laser (Spectra Physics Mai Tai). While one would normally prefer a CW laser for this type of experiment, the 80 MHz pulse repetition rate of this laser is so much faster than the modulation of the magnetic field and response time of the electronics (hundreds of Hz) that the pulsed nature of the signal need not be taken into account. Because the wavelength of this laser is tunable over a range that overlaps the bandgap of the crystal, it allows us to measure a Faraday rotation spectrum, partially inside and partially outside of the band gap, without having to rotate the sample. The experimental setup remains mostly the same as in Figure 8, with a different laser and the sample is kept perpendicular to the beam instead of rotated. The results from this experiment (Figure 10) are in good agreement with those using angular dependence, i.e. the rotation lowers in the area of the band gap. In this experiment, the background rotation for the glass substrate was not measured separately, and it is opposite to that caused by the superparamagnetic particles. This explains why the curve for the crystal with magnetic nanoparticles is lower than that without them. It also demonstrates the significant influence these particles have, as a small addition to a photonic crystal layer mere microns thick (Figure 5) is sufficient to compensate about half of the effect from a 1 mm thick glass substrate.

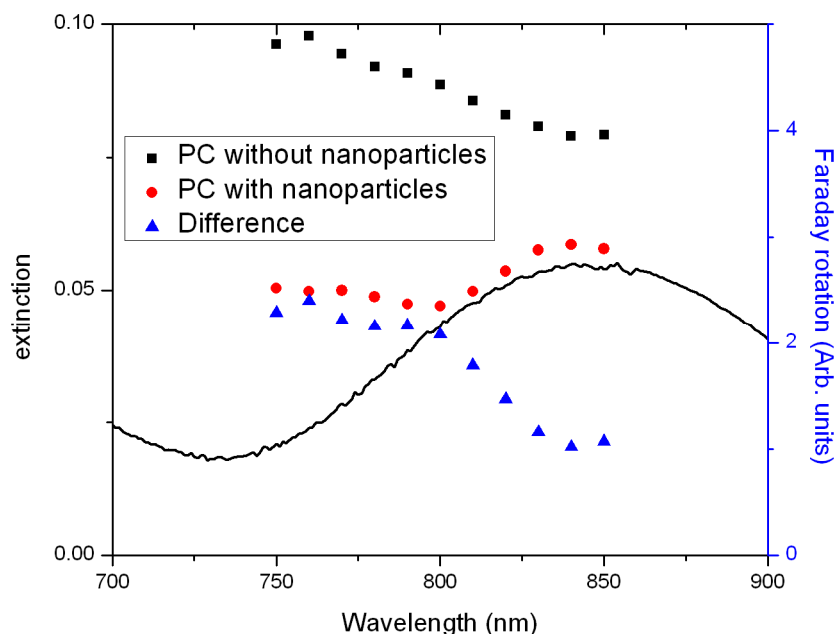


Fig. 10. Results from Faraday rotation measurements in the range of 750 to 850 nm, using a tunable laser on the same photonic crystals as in Figure 9, with the sample perpendicular to the laser beam. We show results for the photonic crystals with and without superparamagnetic nanoparticles, as well as the difference between the two, which clearly shows that those particles have the biggest effect outside of the band gap.

#### 4. CONCLUSION

We have developed a successful strategy towards colloidal photonic crystals with combined optical and magnetic functionality derived from nanoscale engineering of these two properties at different length scale. Enhanced magneto-optic properties were imparted by the synthesis of small (< 20 nm) magnetic maghemite nanoparticles. Optical band gap properties were induced by the convective self-assembly of large (>200 nm) transparent monodisperse silica nanospheres. Insertion of the small magnetic particles after the fabrication of the photonic crystal ensures retention of the good long-range ordering which is essential for the photonic band gap upon imparting magnetic functionality. Comparative Faraday rotation measurements confirm the effect of the magnetic particles in a photonic crystal towards enhancing and tuning magnetic interactions in photonic crystals. Further study and theoretical analysis will be needed in order to better understand the interaction between these materials and light near and in the photonic band gap, but a clear positive effect of the presence of the magnetic particles for Faraday rotation in colloidal photonic crystals has been observed.

#### 5. ACKNOWLEDGEMENTS

The authors thank the Research Fund of the KULeuven for financial support through GOA2006/2 and GOA2006/3, ZWAP 4/07. The Fonds voor Wetenschappelijk Onderzoek Vlaanderen is thanked for a postdoctoral fellowship for R. A. L. V. and for grant G.0458.06. INPAC is thanked for a postdoctoral grant for B. K. The authors warmly acknowledge J. Chen and R. Pitschke (MPI KGF, Golm, Germany) for TEM images, and Thomas Eckert (RWTH Aachen University, Aachen, Germany) for SAXS measurements and useful discussions.

#### REFERENCES

- [1] Lu, A.-H., Salabas, E. L. and Schüth, F., "Magnetic nanoparticles: Synthesis, protection, functionalization, and application," *Angew. Chem. Int. Ed.* 46(8), 1222-1244 (2007).

- [2] Gupta, A. K. and Gupta, M., "Synthesis and surface engineering of iron oxide nanoparticles for biomedical applications," *Biomaterials*, 26(18), 3995-4021 (2005).
- [3] Li, Z., Wei, L., Gao, M. Y. and Lei, H., "One-pot reaction to synthesize biocompatible magnetite nanoparticles," *Adv. Mater.* 17(8), 1001-1005 (2005).
- [4] Hyeon, T., "Chemical synthesis of magnetic nanoparticles," *Chem. Commun.* 8, 927-934 (2003).
- [5] Lu, A.-H., Schmidt, W., Matoussevitch, N., Bönnermann, H., Spliethoff, B., Tesche, B., Bill, E., Kiefer, W. and Schüth, F., "Nanoengineering of a magnetically separable hydrogenation catalyst," *Angew. Chem. Int. Ed.* 43(33), 4303-4306 (2004).
- [6] Tsang, S. C., Caps, V., Paraskevas, I., Chadwick, D. and Thompsett, D., "Magnetically separable, carbon-supported nanocatalysts for the manufacture of fine chemicals," *Angew. Chem. Int. Ed.* 43(42), 5645-5649 (2004).
- [7] Mornet, S., Vasseur, S., Grasset, F., Verveka, P., Goglio, G., Demourgues, A., Portier, J., Pollert, E. and Duguet, E., "Magnetic nanoparticle design for medical applications," *Prog. Solid State Chem.* 34(2-4), 237-247 (2006).
- [8] Schomig, H., Halm, S., Bacher, G., Forchel, A., Maksimov, A. A., Dorozhkin, P. S., Kulakovskii, V. D., Dobrowolska, M. and Furdyna, J. K., "Nanooptics on single magnetic semiconductor quantum dots," *OSA Trends in Optics and Photonics (TOPS) Vol. 89, Quantum Electronics and Laser Science (QELS), Technical Digest, Postconference Edition (Optical Society of America, Washington, DC 2003)* pp. QThe5 (2003).
- [9] Claesson, E. M., [Magnetic Core-Shell Silica Particles], ISBN 978-90-393-4559-7 Doctoral thesis, Utrecht University, (2007).
- [10] Claesson, E. M. and Philipse, A.P., "Monodisperse magnetizable composite silica spheres with tunable dipolar interactions," *Langmuir* 21(21), 9412-9419 (2005).
- [11] Salgueiriño-Maceira, V., Correa-Duarte, M. A., Spasova, M., Liz-Marzán, L. M. and Farle, M., "Composite silica spheres with magnetic and luminescent functionalities," *Adv. Funct. Mater.* 16(4), 509-514 (2006).
- [12] Parker, A. R. and Martini, N., "Structural colour in animals - simple to complex optics," *Opt. Laser Technol.* 38(4-6), 315-322 (2006).
- [13] Yablonovitch, E., "Inhibited spontaneous emission in solid-state physics and electronics," *Phys. Rev. Lett.* 58(20), 2059-2062 (1987).
- [14] Lopez, C., "Materials aspects of photonic crystals," *Adv. Mater.* 15(20), 1679-1704 (2003).
- [15] Jiang, P., Bertone, J. F., Hwang, K. S., and Colvin, V. L., "Single-crystal colloidal multilayers of controlled thickness," *Chem. Mater.* 11(8), 2132-2140 (1999).
- [16] Wostyn, K., Zhao, Y. X., Yee, B., Clays, K., Persoons, A., de Schaezen, G. and Hellemans, L., "Optical properties and orientation of arrays of polystyrene spheres deposited using convective self-assembly," *J. Chem. Phys.* 118(23), 10752-10757 (2003).
- [17] Szekeres, M., Kamalin, O., Schoonheydt, R. A., Wostyn, K., Clays, K., Persoons, A. and Dekany, I., "Ordering and optical properties of monolayers and multilayers of silica spheres deposited by the Langmuir-Blodgett method," *J. Mater. Chem.* 12(11), 3268-3274 (2002).
- [18] Reculosa, S. and Ravaine, S., "Colloidal photonic crystals obtained by the Langmuir-Blodgett technique," *Appl. Surf. Sci.* 246(4), 409-414 (2005).
- [19] Míguez, H., Meseguer, F., López, C., Blanco, Á., Moya, J. S., Requena, J., Mifsud, A. and Fornés, V., "Control of the photonic crystal properties of fcc-packed submicrometer SiO<sub>2</sub> spheres by sintering," *Adv. Mater.* 10(6), 480-483 (1998).
- [20] Jiang, P. and McFarland, M. J., "Large-scale fabrication of wafer-size colloidal crystals, macroporous polymers and nanocomposites by spin-coating," *J. Am. Chem. Soc.* 126(42), 13778-13786 (2004).
- [21] Mihi, A., Ocana, M. and Miguez, H., "Oriented colloidal-crystal thin films by spin-coating microspheres dispersed in volatile media," *Adv. Mater.* 18(17), 2244-2249 (2006).
- [22] Lyubchanskii, I. L., Dadoenkova, N. N., Lyubchanskii, M. I., Shapovalov, E. A. and Rasing, T., "Magnetic photonic crystals," *J. Phys. D Appl. Phys.* 36(18), R277-R287 (2003).
- [23] Inoue, M., Fujikawa, R., Baryshev, A., Khanikaev, A., Lim, P. B., Uchida, H., Aktsipetrov, O., Fedyanin, A., Murzina, T. and Granovsky, A., "Magnetophotonic crystals," *J. Phys. D Appl. Phys.* 39(8), R151-R161 (2006).
- [24] Figotin, A. and Vitebsky, I., "Nonreciprocal magnetic photonic crystals," *Phys. Rev. E* 63(6), 066609 (2001).
- [25] Biswas, R., Sigalas, M. M., Subramania, G. and Ho, K.-M., "Photonic band gaps in colloidal systems," *Phys. Rev. B* 57(7), 3701-3705 (1998).
- [26] Sözüer, H. S., Haus, J. W., Inguva, R., "Photonic bands - convergence problems with the plane-wave method," *Phys. Rev. B* 45(24), 13962-13972 (1992).
- [27] Lenz, J. E., "A Review of Magnetic Sensors," *Proc. IEEE* 78(6), 973-989 (1990).

- [28] Postava, K., Pistora, J. and Yamaguchi, T., "Magneto-optic vector magnetometry for sensor applications," *Sens. Actuators, A* 110(1-3), 242-246 (2004).
- [29] Stöber, W, Fink, A. and Bohn, E., "Controlled growth of monodisperse silica spheres in the micron size range," *J. Colloid Interface Sci.* 26(1), 62-69 (1968).
- [30] Baert, K., Libaers, W., Kolaric, B., Vallée, R.A.L., Van der Auweraer, M., Clays, K., Grandjean, D., Di Vece, M., and Lievens, P., "Development of magnetic materials for photonic applications," *J. Nonlinear Opt. Phys. Mater.* 16(3), 281-294 (2007).
- [31] Ding, T., Song, K., Clays, K. and Tung, C.-H., "Fabrication of 3D Photonic Crystals of Ellipsoids: Convective Self-Assembly in Magnetic Field," *Adv. Mater.* 21(19), 1936-1940 (2009).
- [32] Vallée, R.A.L., Baert, K., Kolaric, B., Van der Auweraer, M., and Clays, K., "Nonexponential decay of spontaneous emission from an ensemble of molecules in photonic crystals," *Phys. Rev. B* 76(4) 045113 (2007).
- [33] Wostyn, K., Zhao, Y.X., de Schaetzen, G., Hellemans, L., Matsuda, N., Clays, K. and Persoons, A., "Insertion of a two-dimensional cavity into a self-assembled colloidal crystal," *Langmuir* 19(10), 4465-4468 (2003).
- [34] Vestergaard, B. and Hansen, S., "Application of Bayesian analysis to indirect Fourier transformation in small-angle scattering," *J. Appl. Cryst.* 39, 797-804 (2006).
- [35] Valev, V.K., Wouters, J. and Verbiest, T., "Precise measurements of Faraday rotation using ac magnetic fields," *Am. J. Phys.* 76(7), 626-629 (2008).
- [36] Valev, V.K., Wouters, J. and Verbiest, T., "Differential detection for measurements of Faraday rotation by means of ac magnetic fields," *Eur. J. Phys.* 29(5), 1099-1104 (2008).
- [37] Taflove, A., and Hagness, S. C., [Computational Electrodynamics: The Finite-Difference Time-Domain Method, third ed.], Artech: Norwood, MA, (2005).
- [38] Farjadpour, A., Roundy, D., Rodriguez, A., Ibanescu, M., Bermel, P., Joannopoulos, J. D., Johnson, S. G., and Burr, G., "Improving accuracy by subpixel smoothing in FDTD," *Optics Letters* 31(20), 2972-2974 (2006).
- [39] Glatter, O., [Neutrons, X-rays and Light: Scattering Methods Applied to Soft Condensed Matter], P. Linder and Th. Zemb (Eds), North-Holland Delta Series (2002).
- [40] Libaers, W., Kolaric, B., Vallée, R. A. L., Wong, J. E., Wouters, J., Valev, V. K., Verbiest, T. and Clays, K., "Engineering colloidal photonic crystals with magnetic functionalities," *Colloids Surf., A* 339(1-3), 13-19 (2009).